Distributed Secondary Control for DC Microgrid Applications with Enhanced Current Sharing Accuracy

Lu, Xiaonan; Guerrero, Josep M.; Sun, Kai

Published in:
Proceedings of the 2013 IEEE International Symposium on Industrial Electronics (ISIE)

DOI (link to publication from Publisher):
10.1109/ISIE.2013.6563742

Publication date:
2013

Document Version
Early version, also known as pre-print

Distributed Secondary Control for DC Microgrid Applications with Enhanced Current Sharing Accuracy

Xiaonan Lu[1] Josep M. Guerrero[2] Kai Sun[1]

1. State Key Lab of Power Systems, Department of Electrical Engineering, Tsinghua University, Beijing, China

2. Department of Energy Technology, Aalborg University, Aalborg, Denmark

***Abstract* – With the consideration of line resistances in a dc microgrid, the current sharing accuracy is lowered down, since the dc output voltage cannot be exactly the same for different interfacing converters. Meanwhile, the dc bus voltage deviation is involved by using droop control. In this paper, a distributed secondary control method is proposed. Droop control is employed as the primary control method for load current sharing. Meanwhile, the dc output voltage and current in each module is transferred to the others by the low bandwidth communication (LBC) network. Average voltage and current controllers are used locally as the distributed secondary controllers in each converter to enhance the current sharing accuracy and restore the dc bus voltage simultaneously. All the controllers are realized locally and the LBC system is only used for changing the data of dc voltage and current. Thus, a decentralized control diagram is accomplished and the requirement of distributed configuration in a microgrid is satisfied. The experimental validation based on a 2×2.2 kW prototype was implemented to demonstrate the proposed approach.**

***Index Terms* – Droop control; secondary control; voltage deviation; current sharing accuracy; dc microgrid; low bandwidth communication**

I. INTRODUCTION

In order to integrate different kinds of renewable energy sources and electrify the remote area, the concept of microgrid was proposed several years ago [1]. Since the utility power system relies on ac form, most literatures on this topic are focusing on ac microgrid [2-6]. However, various sustainable energy sources and loads have natural dc coupling, e.g. photovoltaic (PV) modules, batteries, LEDs and so on. It is more efficient to connect them directly and form a dc microgrid by using dc-dc converters without the ac-dc or dc-ac transformation. Therefore, the overall system efficiency can be enhanced. Meanwhile, in dc microgrids, there is no reactive power and harmonics, so higher power quality can be obtained compared to ac systems [7-11]. Hence, there is a growing awareness and concern on dc microgrids nowadays.

Since renewable energy sources are decentralized connected to the common bus in a microgrid, their interfacing converters are connected in parallel. Power electronics interfacing converter control is a key issue in the operation of a microgrid, especially for the load power sharing between different modules [12-15]. Various control methods were proposed to reach proper power sharing in a parallel converter system, e.g. master-slave control, circular-current-chain (3C) control, etc [16-17]. In order to satisfy the requirement of distributed configuration, droop control without communication or with low bandwidth communication (LBC) is commonly accepted as an efficient power sharing method in a microgrid [18].

In a droop-controlled microgrid, the power sharing method is realized by linearly reducing the voltage reference as the output power increases [18]. Although droop control is widely employed as a decentralized method for load power sharing, its limitation should be noticed. Considering the line impedance, the output power sharing accuracy is lowered down. In an ac microgrid, if the inverters are connected to the point of common coupling (PCC) through inductive line impedance, *P-f* and *Q-E* droop control methods are employed. The active power sharing accuracy can be guaranteed since it is based on the frequency of ac output voltage and the frequencies are the same throughout the microgrid. However, the reactive power sharing accuracy may be lowered down since it is based on the amplitude of output voltage and the amplitudes in the ac side are not exactly the same because of different line impedances [19-22]. Similar analysis can be obtained if the interfacing inverters are connected to the PCC through resistive line impedance and *P-E* and *Q-f* droop methods are used. To enhance the reactive power sharing accuracy in the microgrid with inductive line impedance, several methods were proposed. The concept of virtual impedance was proposed in [19] to match the unequal line impedance. Literature [20] presented a compensation method by using the remote voltage signal and employing an integrator term in the conventional *Q-V* droop control. In literature [21], the voltage amplitude in *Q-V* droop control was replaced by $\dot{V}$, which representing the time rate of the change of the voltage magnitude. In [22], the voltage drop across the impedance was estimated in the grid-connected operation in order to reach the modified slope in the *Q-V* droop control.

In a dc microgrid, the output voltage of each interfacing converter is also affected by different line resistances. Therefore, since droop control is accomplished by the linear relationship between dc output voltage and current, the load

sharing accuracy is lowered down if the line resistance is taken into account. Meanwhile, except for the problem of current sharing accuracy, since droop control is realized by reducing the dc output voltage reference, the voltage deviation is involved. A centralized secondary controller was proposed in [18] to eliminate the voltage deviation. However, if there is a failure in the additional centralized controller, the function of voltage restoration cannot be achieved. Literature [23] presented a control scheme based on the average value of the dc output current in each of the converters. This method is useful for restore the dc bus voltage, while the effect of the enhancement of current sharing accuracy was not obvious enough. This is because that only the average value of each dc output current was considered, while the dc output current was not individually controlled.

In this paper, a LBC based distributed secondary control method is proposed for dc microgrid applications. Particularly, the load power sharing is reached by using droop control in the primary control level. Meanwhile, a hybrid control diagram with average dc current and average dc voltage controllers is employed locally in each converter module in order to enhance the current sharing accuracy and restore the local dc bus voltage simultaneously. Each dc output current is individually controlled in the decentralized controller, so the current sharing accuracy is significantly improved. The LBC system is only used for transferring the dc voltage and current, and all the calculations and controllers are realized locally. Therefore, the control system is suitable for the distributed configuration in a microgrid and the reliability of the system is improved. It can be demonstrated that the proposed control diagram is viable for different communication delays. At the same time, exact proportional load current sharing can be achieved with different line resistances. The detailed model of the proposed control diagram is derived and the system stability is thereby analyzed. The 2×2.2 kW prototype based on dSPACE 1103 was implemented to validate the proposed approach.

II. Proposed Distributed Secondary Control

In the distributed secondary control method, the enhancement of current sharing accuracy and the restoration of local dc bus voltage are realized simultaneously. The LBC system is used for transferring the dc voltage and current in different converters. The comparison of frequently used power sharing method in parallel converter system is shown in Table I, where the advantages of the proposed method can be seen clearly.

The detailed configuration of the proposed method is shown in Fig. 1. The output voltage and current in the dc side of each converter are transferred to the other converters by using LBC network. Then, average voltage and average current controllers are employed in each local control system. For the average voltage controller, the control reference is v_{dc}^{*}, so the output voltage of each converter can be restored. Meanwhile, for the average current controller, the reference value is i_{dci}/k_i (i = 1, 2), where k_i is the current sharing proportion. Hence, proportional output current sharing can be achieved. All the calculation and controllers are achieved locally.

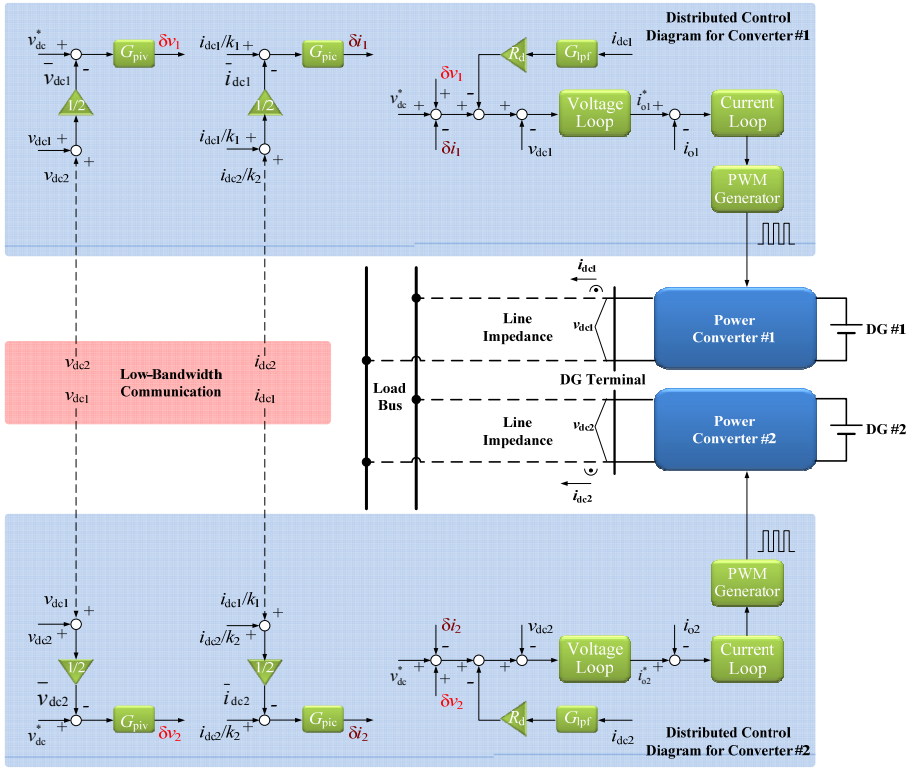

Fig. 1. Detailed configuration of the proposed control system.

TABLE I
COMPARISON OF DIFFERENT POWER SHARING METHODS

Sharing Method	Comm. Dependency	Viability in Microgrids	Sharing Accuracy	DC Vol. Quality
HBC[1] based method	High	Medium	High	High
Conventional droop control	Low	High	Low	Low
Proposed droop control	Low	High	High	High

1. HBC: High bandwidth communication.

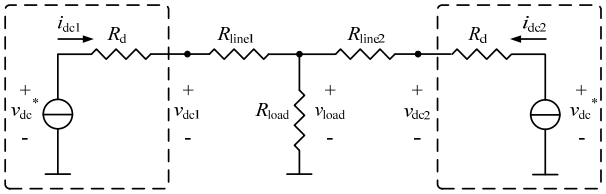

Fig. 2. Simplified model of a two-node dc microgrid.

The stability of the proposed control method is shown as follows. By analyzing the circuit in Fig. 2, it is obtained that

$$i_{dc1} = \alpha_1 \cdot v_{dc1} - \lambda \cdot v_{dc2} \tag{1}$$

$$i_{dc2} = \alpha_2 \cdot v_{dc2} - \lambda \cdot v_{dc1} \tag{2}$$

where

$$\begin{aligned} \alpha_1 &= \frac{R_{line2} + R_{load}}{R_{line1}R_{line2} + R_{line2}R_{load} + R_{line1}R_{load}} \\ \alpha_2 &= \frac{R_{line1} + R_{load}}{R_{line1}R_{line2} + R_{line2}R_{load} + R_{line1}R_{load}} \\ \lambda &= \frac{R_{load}}{R_{line1}R_{line2} + R_{line2}R_{load} + R_{line1}R_{load}} \end{aligned} \tag{3}$$

The detailed model of the control diagram for analyzing the system stability is shown in Fig. 3. The local voltage loop is expressed as

$$G_v = \frac{G_{pi}G_c}{1 + G_{pi}G_c} \tag{4}$$

where G_v, G_{pi} and G_c are the transfer functions of the closed-loop voltage loop, local voltage controller and the local current controller. Here, G_c can be simplified as a delay unit.

In order to ensure the proportional sharing of the dc load current, the target of current sharing is set to

$$\frac{i_{dc1}}{i_{dc2}} = \frac{k_1}{k_2} \tag{5}$$

where k_1 and k_2 represent the current sharing proportion of each converter.

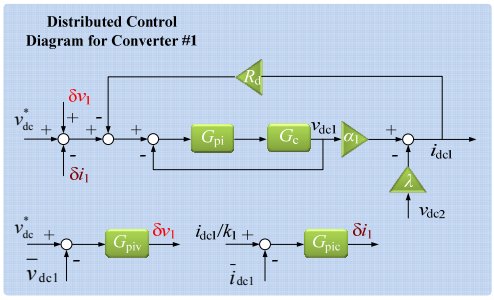

(a)

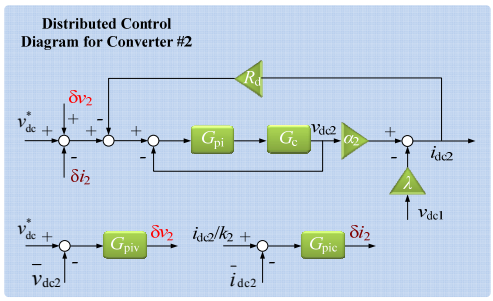

(b)

Fig. 3. Model of the control diagram for analyzing the system stability. (a) Control diagram for Converter #1. (b) Control diagram for Converter #2.

It is obtained from Fig. 3 that

$$\begin{aligned} &v_{dc1} = \\ &[v_{dc}^* + (v_{dc}^* - \bar{v}_{dc1}) \cdot G_{piv} - (i_{dc1}/k_1 - \bar{i}_{dc1}) \cdot G_{pic} - R_{d0}/k_1 \cdot G_{lpf} i_{dc1}] \cdot G_v \end{aligned} \tag{6}$$

$$\begin{aligned} &v_{dc2} = \\ &[v_{dc}^* + (v_{dc}^* - \bar{v}_{dc2}) \cdot G_{piv} - (i_{dc2}/k_2 - \bar{i}_{dc2}) \cdot G_{pic} - R_{d0}/k_2 \cdot G_{lpf} i_{dc2}] \cdot G_v \end{aligned} \tag{7}$$

where $\bar{v}_{dci}$ $(i = 1, 2)$ is the average value of dc output voltage, $\bar{i}_{dci}$ $(i = 1, 2)$ is the average value of dc output current, which are shown as

$$\bar{v}_{dc1} = \frac{v_{dc1} + G_d \cdot v_{dc2}}{2} \tag{8}$$

$$\bar{i}_{dc1} = \frac{i_{dc1}/k_1 + G_d \cdot i_{dc2}/k_2}{2} \tag{9}$$

$$\bar{v}_{dc2} = \frac{G_d \cdot v_{dc1} + v_{dc2}}{2} \tag{10}$$

$$\bar{i}_{dc2} = \frac{G_d \cdot i_{dc1}/k_1 + i_{dc2}/k_2}{2} \tag{11}$$

For Converter #1, v_{dc1} and i_{dc1} are the local variables, while v_{dc2} and i_{dc2} are transferred from Converter #2 through the LBC network. Meanwhile, for Converter #2, v_{dc2} and i_{dc2} are the local variables, while v_{dc1} and i_{dc1} are transferred from Converter #1 through the LBC network. Hence, G_d is involved in (8) – (11) in order to model the communication delay. It is expressed as

$$G_d = \frac{1}{1 + \tau \cdot s} \tag{12}$$

where τ is the communication delay.

At the same time, in (6) and (7), G_{lpf} is the low-pass filter (LPF) in the droop control, which is expressed as

$$G_{lpf} = \frac{\omega_c}{s + \omega_c} \tag{13}$$

where ω_c is the cutting frequency.

Combining (1) – (11), it yields that

$$\begin{aligned} \frac{v_{dc1}}{v_{dc}^*} &= [(1 - G_d)G_{piv} + \frac{(\alpha_2 k_1 + \lambda k_2)(1 + G_d)G_{pic}}{k_1 k_2} \\ &+ 2(\frac{\alpha_2}{k_2} + \frac{\lambda}{k_1})R_{d0}G_{lpf} + \frac{2}{G_v}] \cdot \frac{2k_1^2 k_2^2 G_v^2 (1 + G_{piv})}{A_1 B_2 - A_2 B_1} \end{aligned} \tag{14}$$

$$\begin{aligned} \frac{v_{dc2}}{v_{dc}^*} &= [(1 - G_d)G_{piv} + \frac{(\alpha_1 k_2 + \lambda k_1)(1 + G_d)G_{pic}}{k_1 k_2} \\ &+ 2(\frac{\alpha_1}{k_1} + \frac{\lambda}{k_2})R_{d0}G_{lpf} + \frac{2}{G_v}] \cdot \frac{2k_1^2 k_2^2 G_v^2 (1 + G_{piv})}{A_1 B_2 - A_2 B_1} \end{aligned} \tag{15}$$

where

$$A_1 = k_1k_2G_vG_{piv} + (\alpha_1k_2 + \lambda k_1G_d)G_vG_{pic} + 2k_2\alpha_1R_{d0}G_vG_{lpf} + 2k_1k_2$$
$$A_2 = k_1k_2G_vG_{piv}G_d - (\lambda k_1 + \alpha_1k_2G_d)G_vG_{pic} - 2k_1\lambda R_{d0}G_vG_{lpf}$$
$$B_1 = k_1k_2G_vG_{piv}G_d - (\lambda k_2 + \alpha_2k_1G_d)G_vG_{pic} - 2k_2\lambda R_{d0}G_vG_{lpf}$$
$$B_2 = k_1k_2G_vG_{piv} + (\alpha_2k_1 + \lambda k_2G_d)G_vG_{pic} + 2k_1\alpha_2R_{d0}G_vG_{lpf} + 2k_1k_2$$

TABLE II
SYSTEM PARAMETERS

Item	Symbol	Value	Unit
Reference value of dc output voltage	v_{dc}^*	700	V
Line resistance (Converter #1 Side)	R_{line1}	1	Ω
Line resistance (Converter #2 Side)	R_{line2}	1/6 ~ 6	Ω
Load resistance	R_{load}	200	Ω
Droop coefficient	R_d	6	Ω
LPF cutting frequency	ω_c	126	rads^{-1}
Communication delay	τ	2 ~ 300	ms
Sharing proportion (Converter #1)	k_1	1	1
Sharing proportion (Converter #2)	k_2	1	1

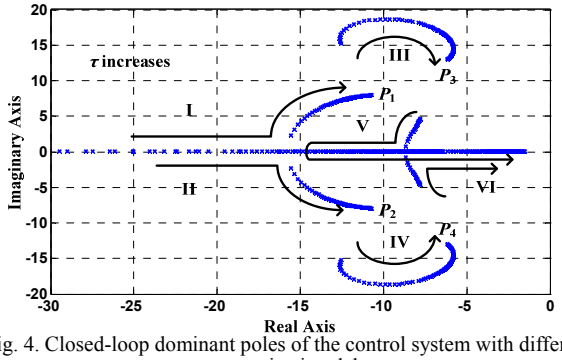

Fig. 4. Closed-loop dominant poles of the control system with different communication delay.

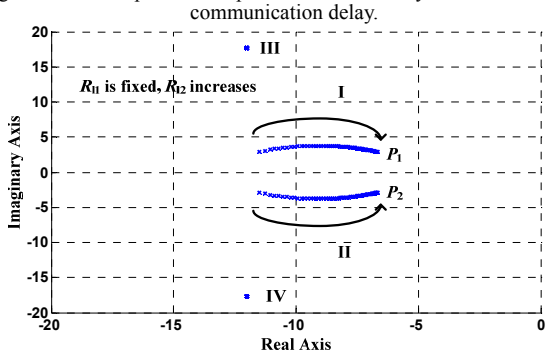

Fig. 5. Closed-loop dominant poles with different line resistances.

Take the control diagram in Converter #1 as an example. The stability of the control system can be tested by analyzing the location of dominant closed-loop poles of (14), with the consideration of different communication delays and line resistances. The system parameters are listed in Table II.

With different communication delay, the closed-loop dominant poles of (14) are shown in Fig. 4. It is seen that the communication delay affects six dominant poles of the control system. As the communication delay τ increases, all of the above poles move towards the imaginary axis. Among different traces of the above dominant poles, Trace I, II, III, and IV are finally terminated at the Point P_1, P_2, P_3 and P_4, respectively. Trace V and VI are gradually extended to the imaginary axis, which challenges the system stability. However, even though τ is as large as 0.3 s, the six dominant poles are located on the left half of the plane. Hence, the stability of the LBC based control system can be guaranteed.

With different line resistances, the closed-loop dominant poles are shown in Fig. 5. Here, the value of R_{line1} is fixed, while the value of R_{line2} changes in order to test the stability of the control system in different conditions. The line resistance R_{line1} is set to 1 Ω and the range of R_{line2} varies from 1/6 Ω to 6 Ω. Therefore, the situations of $R_{line1} \geq R_{line2}$ and $R_{line1} < R_{line2}$ are taken into account. It is seen from Fig. 5 that the line resistance affects two dominant poles of the control system. As R_{line2} increases, the two dominant poles move towards the imaginary axis, while the traces are finally terminated at the points of P_1 and P_2. Therefore, the system stability can be ensured with different line resistances.

IV. EXPERIMENTAL VALIDATION

A 2×2.2 kW prototype with two parallel converters is implemented in order to validate the proposed control system. The system parameters are the same as those shown in Table II. The dc output voltage and current waveforms are exhibited to the performance of the control system. With the proposed method, the dc voltage deviation caused by droop control can be eliminated and the dc output current sharing accuracy can be enhanced at the same time. Meanwhile, the effect of different communication delays and line resistances are taken into account.

A. Effect of different communication delays

Since the proposed control system is implemented based on LBC, different communication delays are tested. The communication delays are selected to 20 ms and 1 s, respectively. The corresponding dc output voltage and current waveforms are shown in Fig. 6 and Fig. 7. Here, R_{line2} is set to 4 Ω and the load current is equally shared.

It is fount from Fig. 6 that with the proposed method, the dc voltage is restored to its reference value and the current sharing accuracy is enhanced when the distributed secondary control turns active. When the communication delay is set to 20 ms, the overshoot and oscillation of the dc output waveforms are acceptable. When the delay is selected as large as 1 s, the control system becomes instable. As shown in Fig. 7, the higher oscillation is found in the dc output voltage waveform, which exceeds the acceptable operation range. Hence, it is concluded that with higher communication delay, it is much harder to keep the control system stable. However, even though the delay is selected as the same as the line period, the output performance is still acceptable. As a result, the viability of the LBC based control diagram is validated.

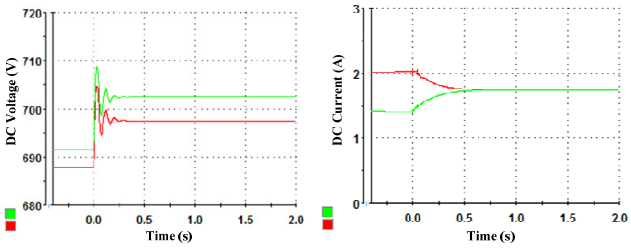

(a) (b)

Fig. 6. Transient waveforms when the LBC based control method turns active (communication delay: 20 ms).
(a) DC voltage restoration. (b) Current sharing accuracy enhancement.

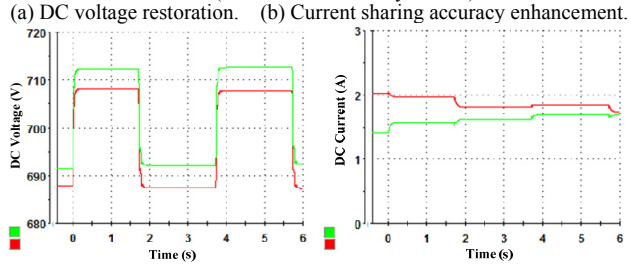

(a) (b)

Fig. 7. Transient waveforms when the LBC based control method turns active (communication delay: 1 s).
(a) DC voltage restoration. (b) Current sharing accuracy enhancement.

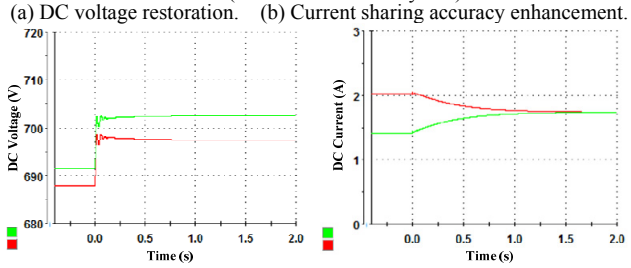

(a) (b)

Fig. 8. Transient waveforms when the LBC based control method turns active (R_{line1} = 1 Ω, R_{line2} = 4 Ω).
(a) DC voltage restoration. (b) Current sharing accuracy enhancement.

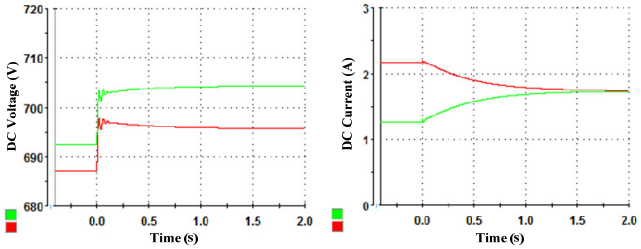

(a) (b)

Fig. 9. Transient waveforms when the LBC based control method turns active (R_{line1} = 1 Ω, R_{line2} = 8 Ω).
(a) DC voltage restoration. (b) Current sharing accuracy enhancement.

B. Effect of different line resistances

In order to further demonstrate the applicability of the control system, different line resistances are tested. Here, R_{line1} is fixed to 1 Ω and R_{line2} is set to 4 Ω and 8 Ω, respectively. The corresponding dc output voltage and current waveforms are shown in Fig. 8 and Fig. 9. Here, equal current sharing is selected as the target of load sharing in the two-node dc microgrid. It is seen that with different line resistances the proposed control system is still valid for dc voltage restoration and current sharing accuracy enhancement.

V. Conclusion

In this paper, a distributed secondary control method with the function of the current sharing accuracy enhancement for dc microgrids is proposed. Particularly, additional average voltage and average current controllers are employed in order to enhance the load current sharing accuracy and restore the local dc output voltage. All the controllers are achieved locally and the required dc voltage and current are transferred to each other through the LBC network. Hence, decentralized control system is realized, which meets the distributed configuration of microgrids. The model of the proposed control system is reached and its stability is thereby discussed. It is demonstrated that even though the communication delay is equal to the several line periods, the stability of the control system can be also guaranteed. At the same time, the viability of the proposed control diagram is ensured with different line resistances. The steady state performance is also carried out in order to derive the quantitative error assessment of the proposed method. The proposed approach is verified by experimental results from a 2×2.2 kW prototype with dSPACE 1103.

Acknowledgement

The authors would like to appreciate the financial support from the National Natural Science Foundation of China (51177083).

References

[1] R. Lasseter, A. Akhil, C. Marnay, J. Stevens, et al, "The certs microgrid concept - white paper on integration of distributed energy resources," *Technical Report*, U.S. Department of Energy, 2002.

[2] J. He and Y. W. Li, "An enhanced microgrid load demand sharing strategy," *IEEE Trans. Power Electron.*,vol. 27, no. 9, pp. 3984-3995, 2012.

[3] Y. W. Li and C. N. Kao, "An accurate power control strategy for power-electronics-interfaced distributed generation units operating in a low-voltage multibus microgrid," *IEEE Trans. Power Electron.*, vol. 24, no. 12, pp. 2977-2988, 2009.

[4] Q. C. Zhong, "Robust droop controller for accurate proportional load sharing among inverters operated in parallel," *IEEE Trans. Ind. Electron.*, vol. 60, no. 4, pp. 1281-1290, 2013.

[5] N. Pogaku, M. Prodanović and T. C. Green, "Modeling, analysis and testing of autonomous operation of an inverter-based microgrid," *IEEE Trans. Power Electron.*, vol. 22, no. 2, pp. 613-625, 2007.

[6] J. C. Vasquez, J. M. Guerrero, A. Luna, et al, "Adaptive droop control applied to voltage-source inverters operation in grid-connected and islanded modes," *IEEE Trans. Ind. Electron.*, vol. 56, no. 10, pp. 4088-4096, 2009.

[7] D. Dong, I. Cvetkovic, D. Boroyevich, W. Zhang, et al, "Grid-interface bi-directional converter for residential DC distribution systems – part one: high-density two-stage topology," *IEEE Trans. Power Electron.*, vol. 28, no. 4, pp. 1655-1666, 2013.

[8] L. Xu and D. Chen, "Control and operation of a DC microgrid with variable generation and energy storage," *IEEE Trans. Power Del.*, vol. 26, no. 4, pp. 2513-2522, 2011.

[9] K. Sun, L. Zhang, Y. Xing and J. M. Guerrero, "A distributed control strategy based on DC bus signaling for modular photovoltaic generation systems with battery energy storage," *IEEE Trans. Power Electron.*, vol. 26, no. 10, pp. 3032-3045, 2011.

[10] H. Kakigano, Y. Miura and T. Ise, "Low-voltage bipolar-type DC microgrid for super high quality distribution," *IEEE Trans. Power Electron.*, vol. 25, no. 12, pp. 3066-3075, 2010.

[11] X. She, A. Q. Huang, S. Lukic and M. E. Baran, "On integration of solid-state transformer with zonal DC microgrid," *IEEE Trans. Smart Grid*, vol. 3, no. 2, pp. 975-985, 2012.

[12] F. Blaabjerg, Z. Chen and S. B. Kjaer, "Power electronics as efficient interface in dispersed power generation systems," *IEEE Trans. Power*

Electron., vol. 19, no. 5, pp. 1184-1194, 2004.

[13] J. M. Carrasco, L. G. Franquelo, J. T. Bialasiewicz, et al, "Power-electronic systems for the grid integration of renewable energy sources: a survey," *IEEE Trans. Ind. Electron.*, vol. 53, no. 4, pp. 1002-1016, 2006.

[14] J. M. Guerrero, M. Chandorkar, T. L. Lee and P. C. Loh, "Advanced control architectures for intelligent microgrids – Part I: decentralized and hierarchical control," *IEEE Trans. Ind. Electron.*, vol. 60, no. 4, pp. 1254-1262, 2013.

[15] J. M. Guerrero, P. C. Loh, T. L. Lee and M. Chandorkar, "Advanced control architectures for intelligent microgrids – Part II: power quality, energy storage, and AC/DC microgrids," *IEEE Trans. Ind. Electron.*, vol. 60, no. 4, pp. 1263-1270, 2013.

[16] J. Rajagopalan, K. Xing, Y. Guo and F. C. Lee, "Modeling and dynamic analysis of paralleled dc/dc converters with master-slave current sharing control," *in Proc. APEC*, 1996, pp.678-684.

[17] T. F. Wu, Y. K. Chen and Y. H. Huang, "3C strategy for inverters in parallel operation achieving an equal current distribution," *IEEE Trans. Ind. Electron.*, vol.47, no.2, pp.273-281, 2000.

[18] J. M. Guerrero, J. C. Vasquez, J. Matas, L. G. Vicuña, et al, "Hierarchical control of droop-controlled AC and DC microgrids - a general approach toward standardization," *IEEE Trans. Ind. Electron.*, vol. 58, no. 1, pp. 158-172, 2011.

[19] J. M. Guerrero, L. G. de Vicuna, J. Matas, M. Castilla, et al, "Output impedance design of parallel-connected UPS inverters with wireless load-sharing control," *IEEE Trans. Ind. Electron.*, vol. 52, no. 4, pp. 1126–1135, 2005.

[20] C. K. Sao and P. W. Lehn, "Autonomous load sharing of voltage source converters," *IEEE Trans. Power Del.*, vol. 20, no. 2, pp. 1009–1016, 2005.

[21] C. T. Lee, C. C. Chu and P. T. Cheng, "A new droop control method for the autonomous operation of distributed energy resource interface converters," IEEE Trans. Power Electron., vol. 28, no. 4, pp. 1980-1993, 2013.

[22] Y. W. Li and C. N. Kao, "An accurate power control strategy for power-electronics-interfaced distributed generation units operating in a low-voltage multibus microgrid," *IEEE Trans. Power Electron.*, vol. 24, no. 12, pp. 2977–2988, 2009.

[23] S. Anand, B. G. Fernandes and J. M. Guerrero, "Distributed control to ensure proportional load sharing and improve voltage regulation in low voltage DC microgrids," *IEEE Trans. Power Electron.*, vol. 28, no. 4, pp. 1900-1913, 2013.